Enhanced visible and near-infrared optical absorption in silicon supersaturated with chalcogens

Si H. Pan,[1] Daniel Recht,[2] Supakit Charnvanichborikarn,[3] James S. Williams,[3] and Michael J. Aziz[2,a)]

[1]*Martin A. Fisher School of Physics, Brandeis University, Waltham, Massachusetts 02453, USA*
[2]*Harvard School of Engineering and Applied Sciences, Cambridge, Massachusetts 02138, USA*
[3]*Department of Electronic Materials Engineering, Research School of Physics and Engineering, The Australian National University, Canberra ACT 0200, Australia*

We show that single-crystal silicon supersaturated with sulfur (S), selenium (Se), or tellurium (Te) displays a substantially enhanced absorption coefficient for light with wavelengths of 400 to 1600 nm. Alloys were prepared in silicon on insulator wafers by ion implantation followed by nanosecond pulsed laser melting. Measurements of the absorption coefficient were made by direct transmission through freestanding thin films and by spectroscopic ellipsometry. © *2011 American Institute of Physics*. [doi:10.1063/1.3567759]

Chalcogen-rich silicon formed by repeated femtosecond or nanosecond pulsed-laser irradiation of silicon wafers in the presence of SF_6 exhibits near-unity below-band-gap absorptance.[1–3] Though this material has been used to improve silicon photodetectors, its spiked surface and complex interior structure complicate the measurement of its optical properties.[4,5] Chalcogen-rich silicon fabricated through ion implantation followed by nanosecond pulsed laser melting also exhibits strong subband-gap absorption but possesses a smooth surface and monocrystalline structure.[6–8] In addition, Tabbal *et al.*[8] observed good rectifying behavior for p-n junctions fabricated by S-implantation and pulsed laser melting of a p-type silicon substrate. These properties suggest applications in thin-film photovoltaics. This work addresses this possibility by reporting the absorption coefficients, over the range of 400–1600 nm, of silicon samples supersaturated with S, Se, and Te by ion implantation followed by pulsed laser melting.

Alloys were formed in the device layer of SOITEC silicon on insulator (SOI) wafers (p-type, B-doped, 13.5–22.5 Ω cm) with a 260 nm Si device layer atop a 1 μm buried oxide on a 625 μm Si substrate. The 260 nm Si layer was ion implanted at room temperature with either 80 keV $^{32}S^+$, 125 keV $^{80}Se^+$, or 120 keV $^{130}Te^+$ to a dose of 1×10^{16} ions/cm^2 or 70 keV Si$^+$ to a dose of 3×10^{15} ions/cm^2 (for preamorphization) followed by 80 keV $^{32}S^+$ to a dose of 1×10^{15} ions/cm^2. All implantation energies were chosen to yield an average ion projected range of approximately 80 nm. Under these conditions, the 1×10^{16} and 3×10^{15} ions/cm^2 doses were sufficient to amorphize roughly the top 200 nm of the 260 nm device layer. The samples were subsequently irradiated with one pulse from a spatially homogenized, pulsed XeCl$^+$ excimer laser (308 nm, 25 ns full width at half maximum, 50 ns pulse duration) with a square spot approximately 3×3 mm^2. A laser fluence of 0.6–0.7 J/cm^2 was chosen empirically to achieve a melt depth in between 200 and 260 nm (i.e., beyond the amorphous layer thickness while still leaving a thin single-crystal silicon layer to seed crystal growth in the subsequent rapid

solidification). Time-resolved reflectivity measurements using a low-power Ar$^+$ ion laser (488 nm) were used to monitor the melt duration.[9,10] Figure 1(a) shows a schematic of samples after ion implantation and pulsed laser melting.

Resolidification was found to occur within a few hundred nanoseconds, such that chalcogen concentrations two to four orders of magnitude higher than equilibrium solubility in silicon remained trapped within the alloy.[11,12] After laser treatment, electron backscattering diffraction on a Zeiss Supra field emission scanning electron microscope was used to confirm the monocrystallinity of each sample. Secondary ion mass spectrometry (SIMS) was performed according the procedure of Bob *et al.*[7] to measure final chalcogen concentrations as shown in Fig. 2. As can be seen from the figure, the retained chalcogen concentration increased with atomic mass, while some Se and Te is segregated to and remains in the near-surface region after resolidification. We note that the SIMS profile for the 1×10^{15} S/cm^2 sample (not shown) is
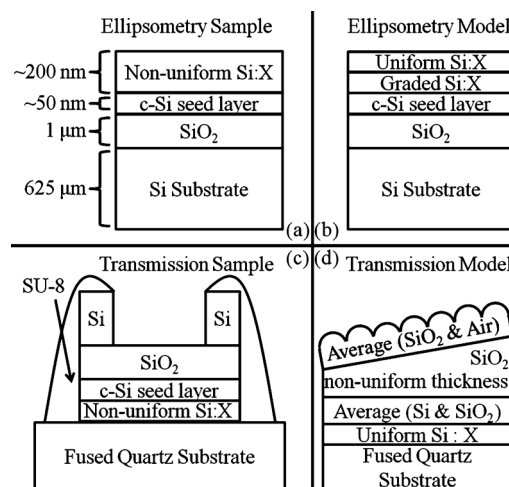

FIG. 1. Schematics illustrating sample structures and how they were modeled. (a) presents a sample structure after pulsed laser melting, where X is the chalcogen species. (b) shows how samples such as the one in (a) were modeled in fitting ellipsometry data. (c) shows a thinned sample. (d) shows how samples such as the one in (c) were modeled in fitting transmission data with "average" layers serving as a model of rough interfaces.
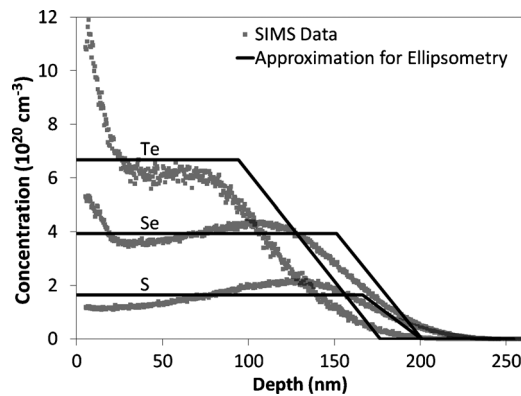
a)Electronic mail: maziz@harvard.edu.

FIG. 2. Experimental SIMS profiles (dots) of S, Se, and Te in SOI samples after implantation to a dose of $1 \times 10^{16}/cm^2$ followed by pulsed laser melting vs the profiles (solid lines) used for fitting the ellipsometry data. The first 5 nm of data were excluded because they were visibly affected by surface transients.
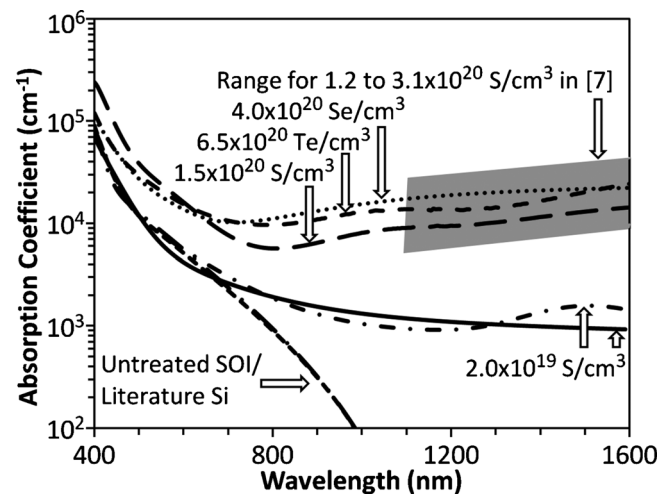

FIG. 3. The optical absorption coefficient of chalcogen-rich silicon, as measured by ellipsometry and reckoned in the region modeled as uniform. The data are compared with those obtained in the same manner from an untreated SOI sample and the literature data on the absorption coefficient of silicon from Ref. 16. A difference of roughly 5 cm^{-1} between the measurement of an untreated SOI sample and the literature data near 1050 nm is not shown in the plot. The range of absorption coefficients measured less precisely in Ref. 7 for samples with S concentrations between 1.2 and 3.1 $\times 10^{20}/cm^3$ (comparable to the 1×10^{16} S/cm^2 samples measured in this work) is also shown.

almost identical to that of the 1×10^{16} S/cm^2 sample but at an order of magnitude lower concentration.

Although spectroscopic ellipsometry is widely used to measure the optical properties of thin films on substrates, interpretation (via numerical fitting) of the raw data produced by an ellipsometer requires one to have some knowledge of the material properties of the film being studied. Because the optical properties of these alloys had never been characterized for photon energies above silicon's band gap, direct transmission through thin films was used to obtain a first, though less precise, measurement. To perform transmission measurements through the alloy layer, it was necessary to remove the 625 μm silicon substrate. We adapted the milling method used by Schmid to create optical windows in heavily doped silicon, replacing the final polishing step with reactive ion etching.[13]

The 625 μm silicon layer was polished to roughly 200 μm in thickness. The sample was then mounted alloy side down onto a fused quartz substrate using SU-8 photoresist so that a 5×5 mm^2 window of bare silicon remained open over the laser-melted area. The sample was then placed on a hot plate at 150 °C for 2 h to evaporate the resist solvent. The remaining 200 μm of Si was removed at a rate of roughly 1 micron per minute by inductively-coupled plasma reactive ion etching in a Surface Technology Systems instrument using a mixture of SF_6, CF_4, and O_2. This recipe etches silicon ~100 times faster than it etches SiO_2. After roughly 4 h of etching, the 5×5 mm^2 of exposed silicon was removed leaving a transparent window consisting of the oxide and alloy layers, shown schematically in Fig. 1(c).

The transmittance of each sample was measured with a Hitachi U-4001 VIS-NIR spectrophotometer equipped with an integrating sphere. The probe beam was focused to fit in the laser-melted region. Due to the challenges inherent in reflectance measurement, there is a long history of using transmittance-only methods to obtain the optical properties of thin films.[14] To extract the optical properties from the transmission data, thinned samples were modeled according to Fig. 1(d). Four layer thicknesses [see Fig. 1(d)] and the absorption coefficients of the alloy layer at wavelengths of 400 nm, 450 nm, 500 nm, 700 nm, 900 nm, 1.1 μm, 1.3 μm, 1.6 μm, 2 μm, and 2.4 μm were used as fitting parameters. The absorption coefficient as a function of wavelength was obtained by smoothly interpolating the values at

the above wavelengths with cubic splines. The refractive index, n, of the alloy layer was assumed to be the same as that of silicon because there was no evidence of reflections from the alloy–silicon interface. Transmittance spectra (not shown) were generated from the model by solving Maxwell's equations recursively at each interface and fit, using a least-squares method, to the measured spectra for wavelengths from 400 to 1600 nm.

Ellipsometry was performed on samples that had not been thinned using a J.A. Woollam *VASE* ellipsometer and raw data were analyzed with its built-in software WVASE32. The ellipsometric parameters Ψ and Δ were measured every 5 nm at 65°, 70°, and 75°. Focusing probes were used for all measurements to reduce the spot size to 200 μm in diameter, ensuring that the probe beam was always within the laser-treated area at all angles. Regression analysis was applied to extract the optical functions from Ψ and Δ. The optical functions were parameterized with an asymmetric-oscillator-based model requiring Kramers–Kronig consistency.[15] In addition, linear grading was used to model the nonuniformity of chalcogen concentration with depth in the implanted layer. Figures 1(a) and 1(b) show schematics of the samples measured in ellipsometry and the way they were modeled respectively. Figure 2, containing the SIMS profiles discussed above, shows the linear compositional grading used to model the concentration profiles. Seeding the oscillator model with the wavelength-dependent absorption coefficient determined from the transmission measurements significantly improved the results of ellipsometry. In addition, because the samples measured in ellipsometry received no treatment after laser melting, we believe the results of ellipsometry to be an accurate representation of the optical properties of these alloys.

Figure 3 shows the wavelength-dependent absorption coefficient of all alloy samples as measured by ellipsometry. Ellipsometry reports the optical properties at the average

chalcogen concentration of the layer modeled as uniform [see Figs. 1(b) and 2]. These concentrations, obtained from SIMS, are reported in Fig. 3. Because they are less than 25 nm thick and thus substantially thinner than the optical penetration depth, the chalcogen-rich regions occurring near the surface of the Se and Te samples are assumed to have no effect other than to raise the average chalcogen concentration. These results are compared with an untreated SOI sample measured by ellipsometry and literature data on the absorption coefficient of silicon.[16] Typically, the results of two samples measured for each case were indistinguishable on a semilog plot and so average values are plotted. The 1×10^{15} S/cm^2 samples were an exception to this and so the results from two samples are plotted separately. In addition, this figure shows the range in which one would expect the absorption coefficient of the highly S-doped samples to fall based on data for comparable sulfur concentrations from the work of Bob *et al.*[7]

Significant enhancement in the absorption coefficient is observed at all wavelengths for samples implanted with chalcogens at 1×10^{16} ions/cm^2 (the top three curves in Fig. 3). The absorption coefficient is roughly an order of magnitude higher than that of hydrated amorphous silicon and comparable to that of cadmium telluride and other compound thin-film solar cell materials.[17] In addition, we note that the results of this work for the 1×10^{16} S/cm^2 samples agree with, extend, and refine the subbandgap measurements of Bob *et al.*[7]

Little structure is observed in the wavelength dependence of absorption for these samples. The absence of peaks or other sharp absorption features suggests a lack of discrete optical transitions in this wavelength range. The slight differences in absorption coefficient between different chalcogen species may be due to several factors. The observed concentration variation caused by laser melting is one such factor, but other effects of rapid solidification may also be important. Different absorption cross sections of different chalcogen species could also play a role.

Some enhancement of the optical absorption is observed in the 1×10^{15} S/cm^2 samples (the middle two curves in Fig. 3) for wavelengths longer than 800 nm. The order of magnitude drop in absorption for these samples relative to the 1×10^{16} S/cm^2 samples is consistent with the linear dependence of absorption on chalcogen concentration observed by Bob *et al.*[7] for concentrations in this range.

In summary, we have measured the absorption coefficient of chalcogen-rich silicon fabricated by ion-implantation followed by pulsed laser melting for the wavelength range from 400 to 1600 nm. Chalcogen doping at about 1 at. % leads to a marked enhancement of the absorption coefficient over the entire wavelength range studied. These results indicate that these alloys have sufficiently high optical absorption coefficients for use in thin-film solar cells. Other important materials properties, such as carrier mobility and lifetime, will be the subject of future research.

[1] C. Wu, C. H. Crouch, L. Zhao, J. E. Carey, R. Younkin, J. A. Levinson, E. Mazur, R. M. Farrell, P. Gothoskar, and A. Karger, Appl. Phys. Lett. **78**, 1850 (2001).
[2] C. H. Crouch, J. E. Carey, J. M. Warrender, E. Mazur, M. J. Aziz, and F. Genin, Appl. Phys. Lett. **84**, 1850 (2004).
[3] C. H. Crouch, J. E. Carey, M. Shen, E. Mazur, and F. Y. Genin, Appl. Phys. A: Mater. Sci. Process. **79**, 1635 (2004).
[4] J. E. Carey, C. H. Crouch, M. A. Sheehy, M. Shen, C. M. Friend, and E. Mazur, Opt. Lett. **30**, 1773 (2005).
[5] Z. Huang, J. E. Carey, M. Liu, X. Guo, E. Mazur, and J. C. Campbell, Appl. Phys. Lett. **89**, 033506 (2006).
[6] T. G. Kim, J. M. Warrender, and M. J. Aziz, Appl. Phys. Lett. **88**, 241902 (2006).
[7] B. P. Bob, A. Kohno, S. Charnvanichborikarn, J. M. Warrender, I. Umezu, M. Tabbal, J. S. Williams, and M. J. Aziz, J. Appl. Phys. **107**, 123506 (2010).
[8] M. Tabbal, T. Kim, J. M. Warrender, M. J. Aziz, B. L. Cardozo, and R. S. Goldman, J. Vac. Sci. Technol. B **25**, 1847 (2007).
[9] M. Tabbal, T. Kim, D. N. Woolf, B. Shin, and M. J. Aziz, Appl. Phys. A: Mater. Sci. Process. **98**, 589 (2010).
[10] R. Reitano, P. M. Smith, and M. J. Aziz, J. Appl. Phys. **76**, 1518 (1994).
[11] R. G. Wilson, J. Appl. Phys. **55**, 3490 (1984).
[12] R. O. Carlson, R. N. Hall, and E. M. Pell, J. Phys. Chem. Solids **8**, 81 (1959).
[13] P. E. Schmid, Phys. Rev. B **23**, 5531 (1981).
[14] R. Swanepoel, J. Phys. E **16**, 1214 (1983).
[15] C. M. Herzinger and B. D. Johs, US Patent No. 5,796,983 (18, August, 1998).
[16] C. M. Herzinger, B. D. Johs, W. A. McGahan, J. A. Woollam, and W. Paulson, J. Appl. Phys. **83**, 3323 (1998).
[17] R. E. I. Schropp and M. Zeman, *Amorphous and Microcrystalline Silicon Solar Cells* (Kluwer Academic, Norwell, MA, 1998).